

Exceptional Near-Infrared Fluorescence Quantum Yields and Excited-State Absorptivity of Highly Conjugated Porphyrin Arrays

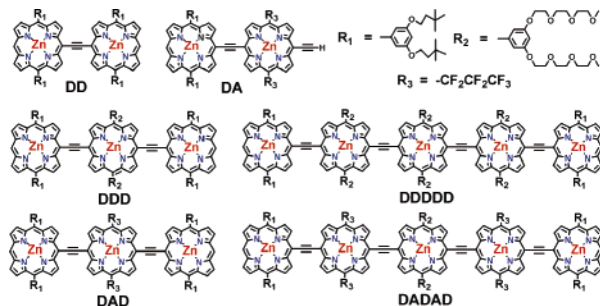
Timothy V. Duncan, Kimihiro Susumu, Louise E. Sinks, and Michael J. Therien*

Department of Chemistry, University of Pennsylvania, Philadelphia, Pennsylvania 19104-6323

Received March 20, 2006; E-mail: therien@sas.upenn.edu

Photonic device applications of low band gap organic materials include photovoltaics, light-emitting diodes, electro-optic modulators, and optical limiters.¹ Each of these applications necessitates an active conjugated material that manifests at least one type of singlet manifold transition ($S_0 \rightarrow S_1$, $S_1 \rightarrow S_0$, or $S_1 \rightarrow S_n$) that possesses unusually large intensity in the near-infrared (NIR). The excited-states of highly π -conjugated, low band gap materials usually manifest shortened excited-state lifetimes due to large magnitude, Franck–Condon mediated, nonradiative decay rate constants, congruent with the energy gap law.² Available NIR-emissive fluorophores are essentially limited to indocyanine green (ICG) and other members of the tricyanocyanine dye family, which possess modest quantum yields^{3a} and the additional undesirable limitations of low chemical and photostability and a marked sensitivity to solvent polarity.^{3b} Likewise, relatively few organic oligomers or polymers have been identified that possess excited singlet states that absorb strongly in the NIR. We show herein that meso-to-meso ethyne-bridged (porphinato)zinc(II) oligomers (PZn_n compounds; Chart 1)⁴ define the first low band gap material platform that simultaneously provides intense, tunable excited-state absorptivity and large NIR fluorescence quantum yields, while overcoming solvent and stability issues associated with charged tricyanocyanine-based NIR laser dyes.

Chart 1. Structures of Bis-, Tris-, and Pentakis(porphinato)zinc(II) (PZn_n) Arrays **DD**, **DA**, **DDD**, **DAD**, **DDDDD**, and **DADAD**



Previous work on PZn_n compounds featuring meso-to-meso ethyne-bridged linkage topologies demonstrate that these compounds manifest low-energy Q-state-derived $\pi-\pi^*$ excited states that are polarized exclusively along the long molecular axis.^{4a,d,e} The optical spectra of highly soluble **DD**-based PZn_n species and their **DA**-derived analogues, which feature alternating electron-rich and electron-poor macrocycles (Chart 1; Figure 1), display lowest energy transitions that gain in intensity and progressively red-shift with increasing numbers of PZn units.^{4a–g} While the electronic structural characteristics of these species have been discussed previously,⁴ it is worth noting that modest PZn_n oligomer lengths give rise to low-energy, high oscillator strength $\pi-\pi^*$ absorptions (Figure 1).

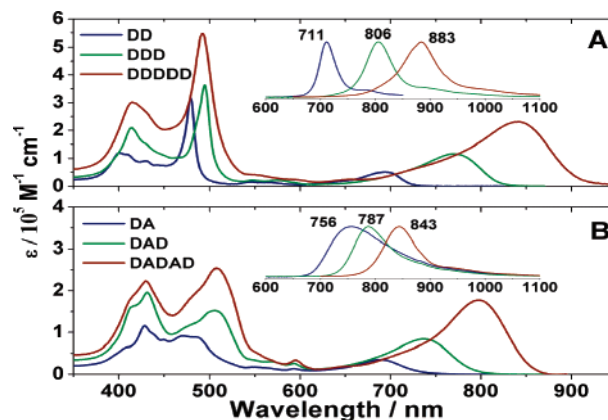


Figure 1. Room-temperature electronic absorption spectra of bis-, tris-, and pentakis[(porphinato)zinc(II)] (PZn_n) arrays based on the **DD** (A) and **DA** (B) structural motifs in THF. Corrected emission spectra, with labeled emission wavelength maxima, are shown in the insets.

Reflecting the extended conjugation in PZn_n , the emission spectra (Figure 1, insets) also red-shift with increasing numbers of conjugated monomeric units, penetrating well into the NIR. Table 1 summarizes the relevant spectroscopic data for these compounds, including the emission quantum yield, ϕ_f , which for all compounds save **DA** range between 14 and 22%. These values are comparable to the highest reported quantum yields for organic chromophores in this energy regime.⁵ The anomalously low **DA** ϕ_f value derives from solvent relaxation processes that augment excited-state polarization;^{4h} such dynamics play no role in determining ϕ_f in symmetric **DA**-based structures (e.g., $\phi_f(\mathbf{DAD}) = 17\%$). Save for **DA**, PZn_n emission bands are narrower than respective $S_0 \rightarrow S_1$ absorption bands, indicating that the final distribution of excited-state conformers is more homogeneous than the respective ground-state distribution.

The trends in the Table 1 ϕ_f data are unusual; for example, the ϕ_f values for **DD** and **DDDDD** are virtually identical ($\sim 15\%$), despite the fact that **DDDDD** emits at 883 nm, 2740 cm^{-1} lower in energy than the **DD** emission maximum; these data contrast the expected energy gap law dependence,² where increasing magnitudes of the S_0-S_1 internal conversion rate constant (k_{ic}) track with diminishing S_0-S_1 energy gaps and, thus, sharply decrease ϕ_f . This unusual dependence of ϕ_f magnitude upon increasing $\lambda_{\text{max}}(S_1 \rightarrow S_0)$ derives in part from the fact that T_1 -state yields decrease with increasing PZn_n conjugation length. Diminished S_1-T_1 intersystem crossing rate constants (k_{isc}) thus serve to partly counterbalance the effect of augmented Franck–Condon mediated internal conversion that typically accompanies S_0-S_1 energy gap reductions (Supporting Information).

Congruent with that observed for **DD** and **DA**,^{4h} fs transient absorption spectroscopy (FTAS) reveals intense NIR $S_1 \rightarrow S_n$ excited-state absorption (ESA) bands for PZn_3 and PZn_5 structures

Table 1. Spectroscopic Parameters of Bis-, Tris-, and Pentakis[(porphinato)zinc(II)] (**PZn_n**) Oligomers in THF

	λ_{\max} ($S_0 \rightarrow S_1$) [nm] ^a	$\epsilon_{\text{g}} @ \lambda_{\max}$ ($S_0 \rightarrow S_1$) [M ⁻¹ cm ⁻¹]	λ_{\max} ($S_1 \rightarrow S_0$) [nm] ^a	ϕ_{f}^b	λ_{\max} ($S_1 \rightarrow S_n$) [nm] ^{a,c}	τ_{f}^d ($\tau_{\text{e}})^e$ [ns]
DD	695 (1085)	51 400	711 (810)	0.16 (0.03)	980 (656)	1.09 (17.6)
DA	688 (1390)	34 000	756 (2170)	0.063 (0.01)	953 (1422)	0.896 (27.5)
DDD	770 (1380)	116 000	806 (875)	0.22 (0.03)	1120 (750)	1.13 (7.32)
DAD	735 (1590)	84 000	787 (1248)	0.17 (0.04)	1070 (1820)	1.11 (9.94)
DDDDD	842 (1563)	230 000	883 (955)	0.14 (0.02)	1325 (1980)	0.45 (3.56)
DADAD	798 (1335)	176 000	843 (987)	0.19 (0.04)	1200 (1960)	0.695 (5.19)

^a Numbers in parentheses are spectral breadths (fwhm) of the respective transitions in units of cm⁻¹. ^b Quantum yields were determined relative to H₂TTP in benzene ($\phi_{\text{f}} = 0.13$); ^c parentetical values represent standard deviations from the mean. ^d Excited-state λ_{\max} values were determined by FTAS 300 fs after photoexcitation. ^e Determined via TCSPC. ^f Parenthetical values are natural radiative lifetimes calculated by the Strickler–Berg method⁷ (see Supporting Information).

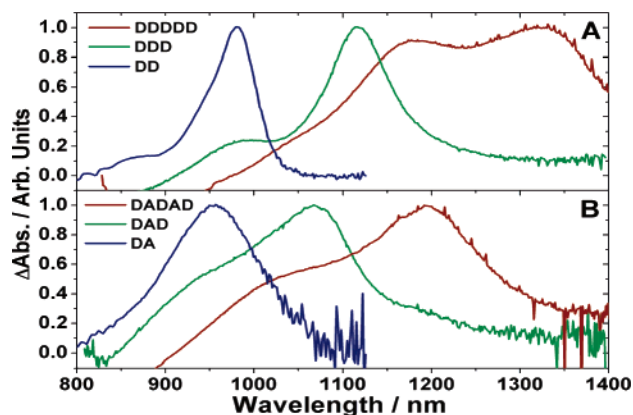


Figure 2. Normalized magic angle NIR transient absorption spectra of the **DD** (A) and **DA** (B) series in THF. The delay times are all ~ 300 fs. Excitation wavelengths were 684 (**DD**), 690 (**DDD**), 775 (**DDDDD**), 685 (**DA**), 690 (**DAD**), and 775 nm (**DADAD**).

(Figure 2). These strong ESA manifolds possess maxima lying 2730–3860 cm⁻¹ lower in energy than the respective fluorescence bands and span a wavelength range of 953–1325 nm (Table 1). Note that **PZn₃** and **PZn₅** species possess broader $S_1 \rightarrow S_n$ absorption manifolds and multiple peak maxima compared to those of the appropriate **PZn₂** benchmark; these excited-state absorptive features derive from augmented conformational heterogeneity that accompanies increasing **PZn_n** conjugation lengths (Supporting Information). The molar extinction coefficients of the $S_1 \rightarrow S_n$ transitions are similar to those tabulated for the x-polarized $S_0 \rightarrow S_1$ absorptions (Table 1; $\sim 10^5$ M⁻¹ cm⁻¹ for **DDDDD**); such broad, intense ESA bands, that extend this deep into the NIR, lack precedent in conjugated emissive structures.

Excited-state lifetimes were determined by both FTAS (τ_{es} , Supporting Information) and time-correlated single-photon counting (TCSPC; τ_{f} , Table 1) with good agreement. The excited-state lifetimes determined from TCSPC vary from 440 ps (**DDDDD**) to 1.13 ns (**DDD**). Trends in ϕ_{f} and τ_{es} (τ_{f}) are consistent with the expected dependences upon the magnitudes of radiative (k_{r}) and nonradiative (k_{nr}) rate processes, where k_{nr} includes contributions due to internal conversion (k_{ic}) and intersystem crossing (k_{isc}) rate constants; for instance, the fact that **DADAD** possesses a larger ϕ_{f} value than **DAD**, despite a shorter excited-state lifetime, derives from a larger magnitude k_{r} , congruent with the Strickler–Berg

relation,⁷ which predicts that k_{r} is proportional to the integrated oscillator strength of the lowest-energy ground-state absorption band. The τ_0 (k_{r}^{-1}) values determined using the Strickler–Berg method can be found in Table 1 and are plotted in Figure S1; these calculated natural lifetimes are consistent with the trends in the experimental data, highlight the close correlation of fluorescence quantum yields with $S_0 \rightarrow S_1$ integrated oscillator strength, and demonstrate a rare if not unique example of broad NIR spectral domain fluorescence energy modulation, where ϕ_{f} magnitudes follow a simple Strickler–Berg relationship (see the Supporting Information section for an expanded discussion of these trends).

In summary, we show that meso-to-meso ethyne-bridged (porphinato)zinc(II) oligomers define exceptional low band gap organic materials that possess both large magnitude NIR $S_1 \rightarrow S_0$ fluorescence quantum yields and substantial $S_1 \rightarrow S_n$ absorptive cross-sections, tunable over a wide 850–1400 nm spectral window. These **PZn_n** species possess fluorescence quantum yields comparable to the highest reported for NIR laser dyes in the 750–900 nm regime; importantly, these emitters do not suffer from commonly cited tricyanocyanine dye drawbacks of poor photostability and substantial ϕ_{f} sensitivity to solvent polarity. These facts, coupled with a Strickler–Berg correlation of $S_0 \rightarrow S_1$ integrated oscillator strength with ϕ_{f} , underscore the potential of these structures in a range of photonic applications.

Acknowledgment. This work was supported by a grant from the ONR (N00014-01-1-0725) and the MRSEC Program of the National Science Foundation (DMR00-79909). T.V.D. and L.E.S. acknowledge respectively Carolyn Hoff Lynch and NIH Ruth L. Kirschstein NRSA Fellowships.

Supporting Information Available: Experimental methods, excited-state dynamical data, and computational details. This material is available free of charge via the Internet at <http://pubs.acs.org>.

References

- (1) (a) Roncali, J. *Chem. Rev.* **1997**, *97*, 173–205. (b) van Mellekom, H. A. M.; Vekemans, J. A. J. M.; Havinga, E. E.; Meijer, E. W. *Mater. Sci. Eng.* **2001**, *32*, 5081–5083. (c) Tsuda, A.; Osuka, A. *Science* **2001**, *293*, 79–82. (d) Ajayaghosh, A. *Chem. Soc. Rev.* **2003**, *32*, 181–191. (e) Sonmez, G.; Meng, H.; Wudl, F. *Chem. Mater.* **2003**, *15*, 4923–4929. (f) Ostrowski, J. C.; Susumu, K.; Robinson, M. R.; Therien, M. J.; Bazan, G. C. *Adv. Mater.* **2003**, *15*, 1296–1300. (g) Chen, M.; Perzon, E.; Andersson, M. R.; Marcinkevicius, S.; Jönsson, S. K. M.; Fahlman, M.; Berggren, M. *Appl. Phys. Lett.* **2004**, *84*, 3570–3572. (h) Wang, X.; Perzon, E.; Delgado, J. L.; de la Cruz, P.; Zhang, F.; Langa, F.; Andersson, M.; Inganäs, O. *Appl. Phys. Lett.* **2004**, *85*, 5081–5083. (i) Shirk, J. S.; Pong, R. G. S.; Flom, S. R.; Heckmann, H.; Hanack, M. *J. Phys. Chem. A* **2000**, *104*, 1438–1449.
- (2) (a) Englman, R.; Jortner, J. *Mol. Phys.* **1970**, *18*, 145–164. (b) Caspar, J. V.; Kober, E. M.; Sullivan, B. P.; Meyer, T. J. *J. Am. Chem. Soc.* **1982**, *104*, 630–632.
- (3) (a) Reindl, S.; Penzkofer, A.; Gong, S. H.; Landthaler, M.; Szeimies, R. M.; Abels, C.; Baumler, W. *J. Photochem. Photobiol., A* **1997**, *105*, 65–68. (b) Lin, Y. H.; Weissleder, R.; Tung, C. H. *Bioconjugate Chem.* **2002**, *13*, 605–610.
- (4) (a) Lin, V. S.-Y.; DiMaggio, S. G.; Therien, M. J. *Science* **1994**, *264*, 1105–1111. (b) Lin, V. S.-Y.; Therien, M. J. *Chem.—Eur. J.* **1995**, *1*, 645–651. (c) Angiolillo, P. J.; Lin, V. S.-Y.; Vanderkooi, J. M.; Therien, M. J. *J. Am. Chem. Soc.* **1995**, *117*, 12514–12527. (d) Kumble, R.; Palese, S.; Lin, V. S.-Y.; Therien, M. J.; Hochstrasser, R. M. *J. Am. Chem. Soc.* **1998**, *120*, 11489–11498. (e) Shediach, R.; Gray, M. H. B.; Uyeda, H. T.; Johnson, R. C.; Hupp, J. T.; Angiolillo, P. J.; Therien, M. J. *J. Am. Chem. Soc.* **2000**, *122*, 7017–7033. (f) Fletcher, J. T.; Therien, M. J. *J. Am. Chem. Soc.* **2002**, *124*, 4298–4311. (g) Susumu, K.; Therien, M. J. *J. Am. Chem. Soc.* **2002**, *124*, 8550–8552. (h) Rubtsov, I. V.; Susumu, K.; Rubtsov, G. I.; Therien, M. J. *J. Am. Chem. Soc.* **2003**, *125*, 2687–2696. (i) Duncan, T. V.; Rubtsov, I. V.; Uyeda, H. T.; Therien, M. J. *J. Am. Chem. Soc.* **2004**, *126*, 9474–9475.
- (5) (a) Birge, R. R.; Duarte, F. J. *Kodak Optical Products*; Kodak Publication: Rochester, New York, 1990; Publication JJ-169B. (b) Kues, H. A.; Benson, R. C. *J. Chem. Eng. Data* **1977**, *22*, 379–383.
- (6) Quimby, D. J.; Longo, F. R. *J. Am. Chem. Soc.* **1975**, *97*, 5111–5117.
- (7) Strickler, S. J.; Berg, R. A. *J. Chem. Phys.* **1962**, *37*, 814–820.

JA0618970